Journal of Mathematical Modeling and Fractional Calculus
https://acspublisher.com/journals/index.php/jmmfc
Received:09-12-2025, **Revised:** 24-12-2026,
Accepted: 01-03-2026, **Published:** 20-06-2026,
https://doi.org/10.48165/jmmfc.2026.3101,3(1),1-20.

Dynamics and control of a fractional fractal Mittag-Leffler $SVEI_1I_2R$ model for Lumpy skin disease

Ankita Dwivedi[a*], Santosh Verma[a]

[a]Guru Ghasidas Vishwavidyalaya (A Central University)Bilaspur - 495009, India.
Corresponding author Email: ankitadwivedi910@gmail.com

Abstract: In this Study we extend the work of Reem K. Alhefthi [12] on Lumpy Skin Disease (LSD) dynamics using symptomatic and asymptomatic measures with a Mittag-Leffler kernel, we propose a fractional fractal Mittag-Leffler $SVEI_1I_2R$ model to capture memory and hereditary effects in disease transmission. The modelŠs dynamical behavior is rigorously analyzed, including local and global stability and the basic reproduction number. We derive conditions for Hopf bifurcation, revealing scenarios that may trigger oscillatory outbreaks. A detailed sensitivity analysis identifies critical epidemiological and control parameters that significantly influence disease spread. Additionally, an optimal control framework based on PontryaginŠs Maximum Principle is developed to minimize infection via vaccination, treatment, and isolation strategies. Numerical simulations demonstrate the profound impact of fractional-order dynamics on epidemic progression, offering insights into the interaction between bifurcation phenomena, parameter sensitivities, and optimal interventions. This study provides a robust, integrated framework for understanding, predicting, and controlling LSD in livestock populations.

Keywords: Fractional fractal Mittag-Leffler, SEVIR model, Hopf bifurcation, Sensitivity analysis, Optimal control, Epidemic dynamics.

1. Introduction

Lumpy Skin Disease (LSD) has emerged as one of the most significant transboundary viral infections affecting cattle populations worldwide. The disease is caused by the Lumpy Skin Disease Virus (LSDV), belonging to the genus *Capripoxvirus* within the family *Poxviridae*. It is characterized by clinical manifestations such as high fever, firm skin nodules, enlarged superficial lymph nodes, edema, and generalized malaise, which together lead to considerable economic losses due to reduced milk yield, infertility, weight loss, and occasionally mortality [12]. Although LSD is not zoonotic and thus poses no direct risk to human health, it significantly affects livestock productivity, animal welfare, and international trade. The transmission of LSD occurs mainly through mechanical vectors such as mosquitoes, biting flies, and ticks, making vector control an essential but challenging aspect of its management. Recent years have witnessed the spread of LSD beyond sub-Saharan Africa to the Middle East, southeastern Europe, and Asia, driven by climatic changes, globalization, and enhanced animal trade. Reports by international health organizations have underscored the necessity of effective surveillance systems, preventive vaccination, and advanced mathematical modeling frameworks to understand and mitigate its spread [12].

Mathematical modeling plays a pivotal role in capturing the dynamics of LSD transmission and control. Classical deterministic models such as SIR, SEIR, and SEQIR frameworks have offered valuable epidemiological insights, yet they often fail to capture the complex memory-dependent and nonlocal effects inherent in real epidemic processes. To overcome these limitations, fractional calculus has gained attention as a powerful tool for modeling infectious diseases, providing an efficient mechanism to represent memory effects and hereditary characteristics in biological systems [1-3, 6, 7]. The introduction of the fractional fractal Mittag-Leffler derivative enables a unified representation of both memory and fractal geometrical structures in the system, offering improved realism in modeling disease persistence and complex temporal behavior [8, 11, 12].

Fractional-order epidemic models have been widely adopted to analyze disease transmission processes where long-term memory and heterogeneous interactions play crucial roles [10, 11,13]. The Caputo and CaputoŰ-Fabrizio derivatives have been particularly useful for modeling non-exponential waiting times and subdiffusive behavior observed in epidemiological data [2, 3]. Furthermore, the Mittag-Leffler kernel has been applied successfully to represent nonlocal and nonsingular memory effects, providing a generalized framework that bridges classical and anomalous diffusion processes [1, 8, 11]. Such fractional-order formulations have significantly enhanced epidemic models' ability to describe persistence, infection waves, and the delayed effects of control interventions [9, 10].

Beyond the descriptive capability of fractional models, incorporating bifurcation theory particularly Hopf bifurcation analysis enables the exploration of periodic and oscillatory dynamics in epidemic systems [9, 16]. Hopf bifurcation provides insight into transitions from stable equilibria to sustained oscillations, corresponding to recurrent or endemic outbreaks. This analytical approach is essential for identifying threshold conditions under which small variations in parameters, such as transmission or recovery rates, can induce large scale epidemic fluctuations. Sensitivity analysis further supports this framework by quantifying the influence of epidemiological parameters on the system's dynamic behavior, helping determine which control variables such as vaccination coverage or vector density have the greatest impact on reducing infection prevalence [10, 15].

The integration of optimal control theory into fractional-order epidemic models offers a powerful means to design efficient intervention strategies. PontryaginŠs Maximum Principle provides a mathematical foundation for determining optimal control profiles that minimize infection prevalence and associated economic losses while balancing costs related to vaccination, treatment, and isolation [10, 17]. Such approaches have been successfully implemented in fractional-order SEIR and SEQIR epidemic models to achieve a balance between health outcomes and resource utilization [10, 13, 18].

Building upon these theoretical advances, the present study proposes a novel fractional-order model for Lumpy Skin Disease dynamics based on the fractional fractal Mittag-Leffler derivative. This derivative captures the nonlocal, memory-dependent, and fractal nature of LSD transmission. The studyŠs main contributions are fourfold: (1) the introduction of the fractional fractal Mittag-Leffler operator into the LSD model to better represent memory effects and heterogeneity [1, 8, 11]; (2) the analysis of Hopf bifurcation phenomena to identify parameter thresholds leading to oscillatory disease behavior[9, 16]; (3) a comprehensive sensitivity analysis to determine the most influential parameters affecting LSD dynamics [10, 15]; and (4) the application of PontryaginŠs Maximum Principle to design optimal control strategies for minimizing infection spread and economic burden [10, 17].

By combining fractional calculus, bifurcation theory, sensitivity analysis, and optimal control into a unified mathematical framework, this work provides both theoretical depth and practical applicability to the study of Lumpy Skin Disease. The use of the fractional fractal Mittag-Leffler derivative allows for realistic modeling of disease persistence and long-term memory effects, while bifurcation and sensitivity analyses yield insights into the nonlinear behavior and stability of the system. Ultimately, this study offers a robust foundation for designing efficient control strategies and advancing our understanding of LSD epidemiology, with potential applications to other vector-borne livestock diseases that exhibit similar nonlocal and memory-driven transmission characteristics [1, 2, 9-11, 16].

1.1. Motivation

Lumpy Skin Disease (LSD), a vector-borne viral infection primarily affecting cattle and buffaloes, poses severe threats to livestock economies worldwide, with outbreaks causing substantial morbidity, mortality, and trade restrictions. Traditional integer-order epidemic models often fail to capture the non-local, memory-dependent nature of disease transmission, particularly in fractal-like biological processes influenced by environmental heterogeneity and long-term immunity waning. Recent work by Alhefthi [12] introduced a fractional model with Mittag-Leffler kernel for LSD dynamics incorporating symptomatic and asymptomatic infections, yet it overlooks fractal structures and advanced bifurcation behaviors essential for predicting oscillatory outbreaks. Motivated by these limitations and the urgent need for memory-aware models in veterinary epidemiology, this study extends the framework to a fractional fractal setting, aiming to elucidate stability thresholds, sensitive parameters, and optimal interventions for LSD control in resource-limited regions like South Asia.

1.2. Novelty

This work introduces the first fractional fractal Mittag-Leffler $SVEI_1I_2R$ model for LSD, integrating fractal dimensionality to realistically depict heterogeneous transmission kernels while preserving memory effects via

the Mittag-Leffler function. Key innovations include:

- rigorous derivation of local/global stability and the basic reproduction number under fractal orders;
- explicit conditions for Hopf bifurcation, uncovering oscillatory dynamics absent in prior models;
- comprehensive sensitivity analysis pinpointing vaccination and isolation as pivotal controls; and
- an optimal control strategy via Pontryagin's Maximum Principle, minimizing infections through time-dependent interventions.

Numerical schemes validate these features, revealing how fractional-fractal orders amplify or dampen bifurcations compared to classical models, providing a novel predictive tool for LSD management.

1.3. Structure of the Paper

The structure of this paper is organized systematically to provide a comprehensive understanding of the modeling, analysis, and control of Lumpy Skin Disease (LSD) under a fractional-order framework. Section 2 presents the formulation of the proposed fractional-order $SVEI_1I_2R$ model, which incorporates the fractional fractal Mittag-Leffler derivative to capture the nonlocal memory and hereditary characteristics of LSD dynamics. In Section 3, the stability of the equilibrium points and the conditions leading to Hopf bifurcation are examined to explore the transition between stable and oscillatory disease states. Section 4 focuses on sensitivity analysis, identifying the most influential epidemiological and control parameters that significantly affect the spread and persistence of the disease. Section 5 introduces optimal control strategies, designed and evaluated using PontryaginŠs Maximum Principle, to minimize infection levels and economic losses through interventions such as vaccination, treatment, and isolation. Section 6 provides an in-depth discussion of the numerical simulations, highlighting the implications of fractional dynamics and control strategies in effectively mitigating LSD outbreaks. Finally, Section 7 concludes the study with key findings, policy insights, and recommendations for future research directions, emphasizing the potential of fractional calculus-based models in improving epidemiological forecasting and control of transboundary livestock diseases.

2. Preliminaries

In this section, we present several essential definitions related to fractional and fractal calculus, which form the mathematical foundation for the proposed Lumpy Skin Disease (LSD) model. These definitions are crucial for understanding the fractional dynamics, memory effects, and hereditary characteristics of the system [1, 2, 4, 6].

1. Definition[Fractal Fractional Derivative, Riemann Liouville Sense [12]] Let $G(t)$ be a continuous and sufficiently differentiable function on the interval (a,b), and let $0 < \xi, \lambda \leq 1$. The fractalŰfractional derivative of order ξ with fractal dimension λ in the RiemannŰLiouville sense is defined as:

$$ {}_0^{FFP}D_t^{\xi,\lambda} G(t) = \frac{1}{\Gamma(n-\xi)} \frac{d}{dt^\lambda} \int_0^t (t-\zeta)^{n-\xi-1} G(\zeta)\, d\zeta, \tag{1} $$

where $n-1 < \xi, \lambda < n$, and $\Gamma(\cdot)$ denotes the Gamma function.

The fractal derivative with respect to ζ is expressed as:

$$ \frac{dG(\zeta)}{d\zeta^\lambda} = \lim_{t\to\zeta} \frac{G(t)-G(\zeta)}{t^\lambda - \zeta^\lambda}. \tag{2} $$

2. Definition[Fractal Fractional Derivative with Exponential Kernel [12]] The fractal fractional derivative of $G(t)$ with an exponentially decaying kernel is defined as:

$$ {}_0^{FFE}D_t^{\xi,\lambda} G(t) = \frac{M(\xi)}{\Gamma(n-\xi)} \frac{d}{dt^\lambda} \int_0^t e^{-\frac{\xi}{1-\xi}(t-\zeta)} G(\zeta)\, d\zeta, \tag{3} $$

where $M(\xi)$ is a normalization function satisfying $M(0) = M(1) = 1$.

3. Definition[Fractal Fractional Derivative with Mittag Leffler Kernel] For $0 < \xi, \lambda \leq 1$, the fractalŰfractional derivative of $G(t)$ using the MittagŰLeffler kernel is defined as:

$$ {}_0^{FFM}D_t^{\xi,\lambda} G(t) = \frac{A(\xi)}{1-\xi} \frac{d}{dt^\lambda} \int_0^t G(\zeta) E_\xi \left(-\frac{\xi}{1-\xi} (t-\zeta)^\xi \right) d\zeta, \tag{4} $$

where $E_\xi(\cdot)$ denotes the MittagŰLeffler function and $A(\xi) = 1 - \xi + \frac{\xi}{\Gamma(\xi)}$ represents the normalization coefficient.

4.Definition[Fractal Fractional Integral [12]] Let $G(t)$ be continuous on (a,b) with $0 < \xi, \lambda \leq 1$. Then, the corresponding fractalŰfractional integral of $G(t)$ of order ξ and fractal dimension λ is given by:

1. **Power law kernel:**

$$ {}_0^{FFP}I_t^{\xi,\lambda} G(t) = \frac{1}{\Gamma(\xi)} \int_0^t (t-\zeta)^{\xi-1} \zeta^{1-\lambda} G(\zeta)\, d\zeta. \tag{5} $$

2. **Exponential kernel:**

$$ {}_0^{FFE}I_t^{\xi,\lambda} G(t) = \frac{\lambda(1-\xi)t^{\lambda-1}}{M(\xi)} G(t) + \frac{\xi\lambda}{M(\xi)} \int_0^t \zeta^{\lambda-1} G(\zeta)\, d\zeta. \tag{6} $$

3. **Mittag Leffler kernel:**

$$ {}_0^{FFM}I_t^{\xi,\lambda} G(t) = \frac{(1-\xi)\lambda t^{\lambda-1}}{A(\xi)} G(t) + \frac{\lambda\xi}{A(\xi)\Gamma(\xi)} \int_0^t (t-\zeta)^{\xi-1} \zeta^{\lambda-1} G(\zeta)\, d\zeta. \tag{7} $$

These generalized operators allow the incorporation of both fractional order and fractal dimension, providing a powerful framework for describing complex biological and epidemiological systems where memory, heterogeneity, and self similarity play a significant role.

3. Model Formulation for Fractional-Order SVEI$_1$I$_2$R System

To comprehensively describe the epidemiological behavior of Lumpy Skin Disease (LSD), we construct a novel and biologically realistic mathematical framework that extends beyond the conventional SVEIR structure by incorporating distinct acute and chronic infection phases. This enhanced framework enables a more accurate understanding of disease progression and facilitates the formulation of effective control and mitigation strategies. The proposed fractional-order $SVEI_1I_2R$ model [12] thus provides deeper insight into both transient outbreak dynamics and long-term disease persistence within livestock populations.

Let the total cattle population at time t be denoted by $N(t)$, consisting of six mutually exclusive compartments: susceptible $S(t)$, vaccinated $V(t)$, exposed $E(t)$, acutely infected $I_1(t)$, chronically infected $I_2(t)$, and recovered $R(t)$. Therefore,

$$ N(t) = S(t) + V(t) + E(t) + I_1(t) + I_2(t) + R(t). $$

Each compartment reflects a biologically meaningful class of individuals that collectively describe the infection dynamics of LSD under fractional-order effects.

The *susceptible class* $S(t)$ represents healthy cattle that are at risk of infection upon contact with infected animals or imperfectly immunized cattle. The *vaccinated class* $V(t)$ comprises animals that have received immunization prior to exposure, thereby achieving partial or complete protection against viral transmission. Upon effective exposure through infected vectors or direct contact, susceptible cattle transition into the *exposed class* $E(t)$, which represents an incubation stage during which the virus replicates without visible clinical manifestations.

Subsequently, individuals in $E(t)$ progress to the *acute infection compartment* $I_1(t)$, symbolizing the early symptomatic stage of the disease. During this stage, the infection is often controllable through timely isolation, medical treatment, and preventive measures. If left unmanaged, the disease advances to the *chronic infection compartment* $I_2(t)$, which denotes a severe and persistent state characterized by reduced recovery potential and increased mortality risk. Finally, individuals recovering from either acute or chronic infection enter the *recovered class* $R(t)$, where they acquire temporary or permanent immunity against reinfection.

This refined compartmentalization framework captures the biological realism of LSD transmission and progression with greater precision. By integrating fractional-order calculus, the model inherently accounts for *memory effects* and *hereditary dynamics*, which are critical in representing disease latency, persistence, and delayed recovery responses. Consequently, the proposed fractional-order $SVEI_1I_2R$ model provides a robust foundation for analyzing stability, bifurcation behavior, and optimal control interventions, ultimately supporting evidence-based strategies for mitigating LSD outbreaks in cattle populations. Let the fractional fractal Mittag-Leffler derivative be denoted by

$$ {}_0^{FFM}D_t^{\xi,\lambda}, $$

where $0 < \xi \leq 1$ and $0 < \lambda \leq 1$.

The model compartments fig.(1, 7) are:

$$ S(t), \quad V(t), \quad E(t), \quad I_1(t), \quad I_2(t), \quad R(t). $$

The fractional-order controlled system is given by

$$ \begin{cases} {}_0^{FFM}D_t^{\xi,\lambda} S(t) = \pi - \theta_1 S I_1 - \rho_1 S I_2 - (\sigma_1 + \mu + \omega_1) S, \\ {}_0^{FFM}D_t^{\xi,\lambda} V(t) = \sigma_1 S - \sigma_2 V I_1 - \rho_2 V I_2 - (\sigma_3 + \mu + \omega_2) V, \\ {}_0^{FFM}D_t^{\xi,\lambda} E(t) = \theta_1 S I_1 + \rho_1 S I_2 + \sigma_2 V I_1 + \rho_2 V I_2 - (\mu + \theta_2) E, \\ {}_0^{FFM}D_t^{\xi,\lambda} I_1(t) = \theta_2 E - (\kappa_1 + \mu + \theta_3 + \theta_4 + \omega_3) I_1, \\ {}_0^{FFM}D_t^{\xi,\lambda} I_2(t) = \theta_4 I_1 - (\kappa_2 + \mu + \theta_5) I_2, \\ {}_0^{FFM}D_t^{\xi,\lambda} R(t) = \theta_3 I_1 + \theta_5 I_2 + \sigma_3 V - \mu R. \end{cases} \tag{8} $$

with initial conditions

$$ S(0) = S_0, \quad V(0) = V_0, \quad E(0) = E_0, \quad I_{1(0)} = I_{1(0)}, \quad I_{2(0)} = I_{2(0)}, \quad R(0) = R_0. $$

Parameter Symbol	**Description**
π	Represents the birth rate
θ_1	Transmission rate from susceptible to exposed via I_1
ρ_1	Transmission rate from susceptible to exposed via I_2
σ_1	Vaccination rate of susceptible cattle
σ_2	Exposure rate of vaccinated cattle due to I_1
ρ_2	Transmission rate from vaccinated to exposed via I_2
σ_3	Recovery/immunity rate of vaccinated cattle
θ_2	Transition rate from exposed to acutely infected
κ_1	Death rate due to acute infection
θ_3	Recovery rate from I_1
θ_4	Transition rate from acute (I_1) to chronic (I_2) infection
κ_2	Death rate due to chronic infection
θ_5	Recovery rate from chronic infection
μ	Natural mortality rate
$\omega_1, \omega_2, \omega_3$	Control variables representing interventions such as vaccination, medication, or isolation

4. Hopf Bifurcation

Theorem 4.1 (Hopf Bifurcation Condition for the Fractional $SVEI_1I_2R$ Model)**.** *Consider the fractional-order $SVEI_1I_2R$ system linearized around the disease-free equilibrium E_0, whose characteristic equation is given by*

$$ \lambda^3 + a_1\lambda^2 + a_2\lambda + a_3 = 0, $$

where

$$\begin{aligned} a_1 &= m + A + B, \\ a_2 &= mA + mB + AB - \theta_2\beta_1, \\ a_3 &= mAB - \theta_2\beta_1 B - \theta_2\theta_4\beta_2, \end{aligned}$$

and the parameters are defined as

$$\begin{aligned} &m = \mu + \theta_2, \qquad A = A_0 + \omega_3, \quad A_0 = \kappa_1 + \mu + \theta_3 + \theta_4, \\ &B = \kappa_2 + \mu + \theta_5, \qquad \beta_1 = \theta_1 S_0 + \sigma_2 V_0, \quad \beta_2 = \rho_1 S_0 + \rho_2 V_0. \end{aligned}$$

Then, the system undergoes a Hopf bifurcation at a critical value $\omega_3 = \omega_3^*$ if the following conditions are satisfied:

1. ***Hopf (classical) condition.*** *The coefficients satisfy*

$$a_1 a_2 = a_3, \qquad \omega^2 = a_2,$$

which leads to the bifurcation equation

$$C_2\omega_3^2 + C_1\omega_3 + C_0 = 0,$$

where

$$\begin{aligned} C_2 &= B + m, \\ C_1 &= 2A_0B + 2A_0m + B^2 + 2Bm + m^2 - \theta_2\beta_1, \\ C_0 &= A_0^2B + A_0^2m + A_0B^2 + 2A_0Bm + A_0m^2 - A_0\theta_2\beta_1 \\ &\quad + B^2m + Bm^2 - m\theta_2\beta_1 + \theta_2\theta_4\beta_2. \end{aligned}$$

The corresponding critical value of the bifurcation parameter is given by

$$\boxed{\omega_3^* = \frac{-C_1 \pm \sqrt{C_1^2 - 4C_2C_0}}{2C_2}}.$$

2. ***Transversality condition.*** *The transversality condition is satisfied whenever*

$$\Re\left(\frac{d\lambda}{d\omega_3}\Big|_{\omega_3=\omega_3^*}\right) \neq 0,$$

where

$$\Re\left(\frac{d\lambda}{d\omega_3}\right) = -\frac{Ba_1 - Bm + a_1m + a_2}{2(a_2 + a_1^2)}.$$

Therefore, a Hopf bifurcation occurs at $\omega_3 = \omega_3^*$ whenever

$$\boxed{a_1(B+m) - Bm + a_2 \neq 0},$$

and all other eigenvalues have negative real parts.

Proof. The characteristic equation of the infected subsystem near the disease-free equilibrium is given by

$$F(\lambda, \omega_3) = \lambda^3 + a_1\lambda^2 + a_2\lambda + a_3 = 0,$$

where a_1, a_2, and a_3 depend on ω_3 through $A = A_0 + \omega_3$. Differentiating implicitly with respect to ω_3 gives

$$\frac{d\lambda}{d\omega_3} = -\frac{\frac{\partial F}{\partial \omega_3}}{\frac{\partial F}{\partial \lambda}},$$

where

$$\frac{\partial F}{\partial \lambda} = 3\lambda^2 + 2a_1\lambda + a_2, \qquad \frac{\partial F}{\partial \omega_3} = \frac{da_1}{d\omega_3}\lambda^2 + \frac{da_2}{d\omega_3}\lambda + \frac{da_3}{d\omega_3}.$$

Since A depends linearly on ω_3, we have

$$\frac{da_1}{d\omega_3} = 1, \qquad \frac{da_2}{d\omega_3} = m + B, \qquad \frac{da_3}{d\omega_3} = mB.$$

Substituting these derivatives into the above expression yields

$$\frac{d\lambda}{d\omega_3} = -\frac{\lambda^2 + (m+B)\lambda + mB}{3\lambda^2 + 2a_1\lambda + a_2}.$$

At the Hopf bifurcation point $\lambda = i\omega$, we have

$$N = -\omega^2 + i(m+B)\omega + mB, \qquad D = -3\omega^2 + i2a_1\omega + a_2.$$

Hence,

$$\Re\left(\frac{d\lambda}{d\omega_3}\right) = \frac{-Ba_2m + 3Bm\omega^2 - 2a_1\omega^2(B+m) + a_2\omega^2 - 3\omega^4}{(-3\omega^2 + a_2)^2 + 4a_1^2\omega^2}.$$

Using the Hopf conditions $\omega^2 = a_2$ and $a_3 = a_1a_2$, the above expression simplifies to

$$\Re\left(\frac{d\lambda}{d\omega_3}\right) = -\frac{Ba_1 - Bm + a_1m + a_2}{2(a_2 + a_1^2)}.$$

The transversality condition requires that the real part of this expression is nonzero. Therefore, a Hopf bifurcation exists if

$$a_1(B+m) - Bm + a_2 \neq 0,$$

and all remaining eigenvalues have negative real parts. This completes the proof. □

Corollary[Fractional Hopf Boundary via Matignon's Criterion] Let the characteristic polynomial of the linearized infected subsystem at the DFE be

$$F(\lambda, \omega_3) = \lambda^3 + a_1(\omega_3)\lambda^2 + a_2(\omega_3)\lambda + a_3(\omega_3) = 0,$$

with a_i as in Theorem 4.1. For the fractional system of order $0 < \xi \leq 1$, the equilibrium lies on the fractional stability boundary when a conjugate pair of roots satisfies Matignon's boundary

$$\arg(\lambda) = \pm\frac{\xi\pi}{2}.$$

Writing

$$\lambda = \rho\, e^{i\frac{\xi\pi}{2}}, \qquad \rho > 0,$$

the fractional Hopf (boundary) conditions are obtained by separating real and imaginary parts of

$$F\big(\rho e^{i\frac{\xi\pi}{2}}, \omega_3\big) = 0,$$

i.e. the system of two real equations

$$\begin{cases} \Re\big(F(\rho e^{i\frac{\xi\pi}{2}}, \omega_3)\big) = 0, \\ \Im\big(F(\rho e^{i\frac{\xi\pi}{2}}, \omega_3)\big) = 0, \end{cases}$$

which determine the boundary pair (ρ, ω_3) (together with a nondegeneracy/transversality condition).

Proof. Substitute $\lambda = \rho e^{i\frac{\xi\pi}{2}}$ into the cubic polynomial and expand:

$$F(\rho e^{i\frac{\xi\pi}{2}}, \omega_3) = \rho^3 e^{i\frac{3\xi\pi}{2}} + a_1\rho^2 e^{i\xi\pi} + a_2\rho e^{i\frac{\xi\pi}{2}} + a_3.$$

Separating real and imaginary parts yields the two scalar equations

$$\rho^3\cos\left(\tfrac{3\xi\pi}{2}\right) + a_1\rho^2\cos(\xi\pi) + a_2\rho\cos\left(\tfrac{\xi\pi}{2}\right) + a_3 = 0,$$

$$\rho^3\sin\left(\tfrac{3\xi\pi}{2}\right) + a_1\rho^2\sin(\xi\pi) + a_2\rho\sin\left(\tfrac{\xi\pi}{2}\right) = 0.$$

These two equations in the unknowns (ρ, ω_3) (recalling $a_i = a_i(\omega_3)$) locate points where a conjugate pair of eigenvalues lies exactly on the Matignon boundary $\arg(\lambda) = \pm\xi\pi/2$.

To obtain a bona fide fractional Hopf bifurcation (crossing of the boundary), one must additionally verify a transversality (nondegeneracy) condition. Differentiate $F(\lambda(\omega_3), \omega_3) = 0$ implicitly with respect to ω_3 and evaluate along the boundary root $\lambda = \rho e^{i\xi\pi/2}$ to check that

$$\Re\left(\frac{d\lambda}{d\omega_3}\right)\Bigg|_{\lambda=\rho e^{i\frac{\xi\pi}{2}}} \neq 0,$$

(or equivalently that the real part of the velocity of the root across the Matignon line is nonzero). If this transversality holds, a conjugate pair of eigenvalues crosses the stability boundary as ω_3 passes through the computed ω_3^* and a fractional Hopf bifurcation occurs. □

Corollary[Elimination of ρ and algebraic condition for ω_3] Let $F(\lambda, \omega_3) = \lambda^3 + a_1(\omega_3)\lambda^2 + a_2(\omega_3)\lambda + a_3(\omega_3)$ be the characteristic polynomial of the infected subsystem as in Theorem 4.1. For the fractional order $0 < \xi \leq 1$, set

$$\lambda = \rho e^{i\frac{\xi\pi}{2}}, \qquad \rho > 0,$$

and denote

$$c_1 = \cos\left(\tfrac{3\xi\pi}{2}\right), \quad s_1 = \sin\left(\tfrac{3\xi\pi}{2}\right),$$
$$c_2 = \cos(\xi\pi), \qquad s_2 = \sin(\xi\pi),$$
$$c_3 = \cos\left(\tfrac{\xi\pi}{2}\right), \quad s_3 = \sin\left(\tfrac{\xi\pi}{2}\right).$$

Separating real and imaginary parts of $F(\rho e^{i\xi\pi/2}, \omega_3) = 0$ yields

$$h(\rho, \omega_3) = \rho^3 c_1 + a_1(\omega_3)\rho^2 c_2 + a_2(\omega_3)\rho c_3 + a_3(\omega_3) = 0, \tag{9}$$
$$f(\rho, \omega_3) = \rho^3 s_1 + a_1(\omega_3)\rho^2 s_2 + a_2(\omega_3)\rho s_3 = 0. \tag{10}$$

Because f has no constant term we factor ρ and exclude the trivial root $\rho = 0$, obtaining the quadratic

$$g(\rho, \omega_3) = \rho^2 s_1 + a_1(\omega_3)\rho s_2 + a_2(\omega_3)s_3 = 0.$$

Eliminating ρ between the cubic $h(\rho, \omega_3)$ and the quadratic $g(\rho, \omega_3)$ is equivalent to requiring that their Sylvester resultant (with respect to ρ) vanishes. Denote this resultant by $\mathrm{Res}_\rho(h, g)$. Then the fractional Hopf boundary condition (with ρ eliminated) is

$$\boxed{\mathrm{Res}_\rho\big(h(\cdot, \omega_3), g(\cdot, \omega_3)\big) \;=\; 0}.$$

Moreover the resultant can be written explicitly as the determinant of the 5×5 Sylvester matrix:

$$\mathrm{Res}_\rho(h, g) = \det \begin{pmatrix} c_1 & a_1 c_2 & a_2 c_3 & a_3 & 0 \\ 0 & c_1 & a_1 c_2 & a_2 c_3 & a_3 \\ s_1 & a_1 s_2 & a_2 s_3 & 0 & 0 \\ 0 & s_1 & a_1 s_2 & a_2 s_3 & 0 \\ 0 & 0 & s_1 & a_1 s_2 & a_2 s_3 \end{pmatrix} = 0.$$

Here each entry a_j is shorthand for $a_j(\omega_3)$. Substituting the explicit forms

$$a_1(\omega_3) = m + (A_0 + \omega_3) + B,$$
$$a_2(\omega_3) = m(A_0 + \omega_3) + mB + (A_0 + \omega_3)B - \theta_2\beta_1,$$
$$a_3(\omega_3) = m(A_0 + \omega_3)B - \theta_2\beta_1 B - \theta_2\theta_4\beta_2,$$

yields a single algebraic equation in ω_3. This equation is, in general, a high-degree polynomial (after expansion) whose real roots in the admissible parameter range give the fractional Hopf candidates ω_3^*.

Remarks on computation. The determinant above is the Sylvester resultant of a cubic and a quadratic in ρ; expanding it gives a (generally high-degree) polynomial in the coefficients $c_1, c_2, c_3, s_1, s_2, s_3$ and $a_1(\omega_3), a_2(\omega_3), a_3(\omega_3)$. Because the a_i depend linearly or quadratically on ω_3, the fully expanded resultant is an explicit polynomial condition

$$P(\omega_3; \xi, \text{model parameters}) = 0,$$

and its real roots yield the bifurcation parameter values. This produces the explicit algebraic equation in ω_3 suitable for root-finding and further analysis. □

5. Sensitivity analysis of the basic reproduction number R_0

Definitions and equilibrium values

At the disease-free equilibrium (DFE) with constant recruitment π,

$$S^* = \frac{\pi}{\sigma_1 + \mu + \omega_1}, \qquad V^* = \frac{\sigma_1 S^*}{\sigma_3 + \mu + \omega_2}.$$

Introduce the compact notation

$$A = \kappa_1 + \mu + \theta_3 + \theta_4 + \omega_3, \qquad B = \kappa_2 + \mu + \theta_5,$$

and the effective transmission quantities

$$\beta_1 = \theta_1 S^* + \sigma_2 V^*, \qquad \beta_2 = \rho_1 S^* + \rho_2 V^*.$$

We use the standard next-generation expression

$$\boxed{R_0 = \frac{\beta_1}{A} + \frac{\theta_4 \beta_2}{AB}}.$$

Normalized sensitivity index

The normalized (relative) sensitivity index of R_0 with respect to a parameter p is

$$S_p^{R_0} = \frac{p}{R_0} \frac{\partial R_0}{\partial p}.$$

Direct derivatives (parameters that appear explicitly in β_i, A, B)

For parameters entering linearly in β_1, β_2, A, B the derivatives are:

(i) θ_1:

$$\frac{\partial R_0}{\partial \theta_1} = \frac{S^*}{A}, \qquad S_{\theta_1}^{R_0} = \frac{\theta_1}{R_0} \cdot \frac{S^*}{A}.$$

(ii) ρ_1:

$$\frac{\partial R_0}{\partial \rho_1} = \frac{\theta_4 S^*}{AB}, \qquad S_{\rho_1}^{R_0} = \frac{\rho_1}{R_0} \cdot \frac{\theta_4 S^*}{AB}.$$

(iii) σ_2:

$$\frac{\partial R_0}{\partial \sigma_2} = \frac{V^*}{A}, \qquad S_{\sigma_2}^{R_0} = \frac{\sigma_2}{R_0} \cdot \frac{V^*}{A}.$$

(iv) ρ_2:

$$\frac{\partial R_0}{\partial \rho_2} = \frac{\theta_4 V^*}{AB}, \qquad S_{\rho_2}^{R_0} = \frac{\rho_2}{R_0} \cdot \frac{\theta_4 V^*}{AB}.$$

(v) θ_4 (appears in numerator and in A):

$$\frac{\partial R_0}{\partial \theta_4} = -\frac{\beta_1}{A^2} + \frac{\beta_2}{AB} - \frac{\theta_4 \beta_2}{A^2 B},$$

hence

$$S_{\theta_4}^{R_0} = \frac{\theta_4}{R_0}\Big(-\frac{\beta_1}{A^2} + \frac{\beta_2}{AB} - \frac{\theta_4 \beta_2}{A^2 B}\Big).$$

(vi) κ_1 (in A):

$$\frac{\partial R_0}{\partial \kappa_1} = -\frac{\beta_1}{A^2} - \frac{\theta_4\beta_2}{A^2 B}, \qquad S^{R_0}_{\kappa_1} = \frac{\kappa_1}{R_0}\Big(-\frac{\beta_1}{A^2} - \frac{\theta_4\beta_2}{A^2 B}\Big).$$

(vii) κ_2 (in B):

$$\frac{\partial R_0}{\partial \kappa_2} = -\frac{\theta_4\beta_2}{AB^2}, \qquad S^{R_0}_{\kappa_2} = \frac{\kappa_2}{R_0}\Big(-\frac{\theta_4\beta_2}{AB^2}\Big).$$

(viii) control ω_3 (in A, same as κ_1):

$$\frac{\partial R_0}{\partial \omega_3} = -\frac{\beta_1}{A^2} - \frac{\theta_4\beta_2}{A^2 B}, \qquad S^{R_0}_{\omega_3} = \frac{\omega_3}{R_0}\Big(-\frac{\beta_1}{A^2} - \frac{\theta_4\beta_2}{A^2 B}\Big).$$

(ix) natural mortality μ: μ enters A, B and S^*, V^*. One may compute it by chain rule (see below).

Chain-rule: parameters that affect S^* and V^* (vaccination and control rates)

Because β_1, β_2 depend on S^*, V^*, which depend on $\sigma_1, \sigma_3, \omega_1, \omega_2, \mu, \pi$, use the chain rule:

$$\frac{\partial R_0}{\partial p} = \frac{1}{A}\Big(\theta_1\frac{\partial S^*}{\partial p} + \sigma_2\frac{\partial V^*}{\partial p}\Big) + \frac{\theta_4}{AB}\Big(\rho_1\frac{\partial S^*}{\partial p} + \rho_2\frac{\partial V^*}{\partial p}\Big),$$

for any p that influences S^*, V^*.

For σ_1 (as a representative example):

$$S^* = \frac{\pi}{\sigma_1 + \mu + \omega_1}, \qquad V^* = \frac{\sigma_1 S^*}{\sigma_3 + \mu + \omega_2},$$

so

$$\frac{\partial S^*}{\partial \sigma_1} = -\frac{\pi}{(\sigma_1 + \mu + \omega_1)^2} = -\frac{S^*}{\sigma_1 + \mu + \omega_1},$$

and

$$\frac{\partial V^*}{\partial \sigma_1} = \frac{S^*}{\sigma_3 + \mu + \omega_2} + \frac{\sigma_1}{\sigma_3 + \mu + \omega_2}\frac{\partial S^*}{\partial \sigma_1}.$$

Thus

$$\frac{\partial R_0}{\partial \sigma_1} = \frac{1}{A}\Big(\theta_1\frac{\partial S^*}{\partial \sigma_1} + \sigma_2\frac{\partial V^*}{\partial \sigma_1}\Big) + \frac{\theta_4}{AB}\Big(\rho_1\frac{\partial S^*}{\partial \sigma_1} + \rho_2\frac{\partial V^*}{\partial \sigma_1}\Big),$$

and finally

$$S^{R_0}_{\sigma_1} = \frac{\sigma_1}{R_0}\frac{\partial R_0}{\partial \sigma_1}.$$

Chain-rule derivatives for $\sigma_3, \omega_1, \omega_2, \mu, \pi$

Recall

$$S^* = \frac{\pi}{D_1}, \qquad V^* = \frac{\sigma_1 S^*}{D_2},$$

where

$$D_1 := \sigma_1 + \mu + \omega_1, \qquad D_2 := \sigma_3 + \mu + \omega_2.$$

Also

$$A := \kappa_1 + \mu + \theta_3 + \theta_4 + \omega_3, \qquad B := \kappa_2 + \mu + \theta_5,$$

and

$$\beta_1 = \theta_1 S^* + \sigma_2 V^*, \qquad \beta_2 = \rho_1 S^* + \rho_2 V^*, \qquad R_0 = \frac{\beta_1}{A} + \frac{\theta_4\beta_2}{AB}.$$

Derivatives of S^* and V^*..

$$\frac{\partial S^*}{\partial \pi} = \frac{1}{D_1} = \frac{S^*}{\pi}, \qquad \frac{\partial S^*}{\partial \omega_1} = -\frac{\pi}{D_1^2} = -\frac{S^*}{D_1},$$
$$\frac{\partial S^*}{\partial \sigma_3} = 0, \qquad \frac{\partial S^*}{\partial \omega_2} = 0,$$
$$\frac{\partial S^*}{\partial \mu} = -\frac{\pi}{D_1^2} = -\frac{S^*}{D_1}.$$
$$\frac{\partial V^*}{\partial p} = \frac{\sigma_1}{D_2}\frac{\partial S^*}{\partial p} + \sigma_1 S^* \frac{d}{dp}\left(\frac{1}{D_2}\right)$$
$$= \frac{\sigma_1}{D_2}\frac{\partial S^*}{\partial p} - \frac{\sigma_1 S^*}{D_2^2}\frac{\partial D_2}{\partial p}.$$

Hence, using $\partial D_2/\partial \sigma_3 = 1$, $\partial D_2/\partial \mu = 1$, $\partial D_2/\partial \omega_2 = 1$ and zero otherwise,

$$\frac{\partial V^*}{\partial \pi} = \frac{\sigma_1}{D_2}\frac{\partial S^*}{\partial \pi} = \frac{\sigma_1}{D_2}\cdot\frac{1}{D_1} = \frac{V^*}{\pi},$$
$$\frac{\partial V^*}{\partial \omega_1} = \frac{\sigma_1}{D_2}\frac{\partial S^*}{\partial \omega_1} = -\frac{\sigma_1 S^*}{D_2 D_1} = -\frac{V^*}{D_1},$$
$$\frac{\partial V^*}{\partial \sigma_3} = -\frac{\sigma_1 S^*}{D_2^2} = -\frac{V^*}{D_2},$$
$$\frac{\partial V^*}{\partial \omega_2} = \frac{\sigma_1}{D_2}\cdot 0 - \frac{\sigma_1 S^*}{D_2^2} = -\frac{V^*}{D_2},$$
$$\frac{\partial V^*}{\partial \mu} = \frac{\sigma_1}{D_2}\frac{\partial S^*}{\partial \mu} - \frac{\sigma_1 S^*}{D_2^2} = -\frac{\sigma_1 S^*}{D_2 D_1} - \frac{V^*}{D_2} = -\frac{V^*}{D_1} - \frac{V^*}{D_2}.$$

($\partial V^*/\partial \pi = V^*/\pi$, $\partial V^*/\partial \omega_1 = -V^*/D_1$, $\partial V^*/\partial \sigma_3 = -V^*/D_2$, $\partial V^*/\partial \omega_2 = -V^*/D_2$, $\partial V^*/\partial \mu = -V^*(1/D_1 + 1/D_2)$.)

Derivative of R_0 via chain rule.. For any parameter p that affects only S^*, V^* (and neither A nor B), we have

$$\boxed{\frac{\partial R_0}{\partial p} = \frac{1}{A}\Big(\theta_1 \frac{\partial S^*}{\partial p} + \sigma_2 \frac{\partial V^*}{\partial p}\Big) + \frac{\theta_4}{AB}\Big(\rho_1 \frac{\partial S^*}{\partial p} + \rho_2 \frac{\partial V^*}{\partial p}\Big).}$$

For μ, which also appears in A and B, include those contributions:

$$\frac{\partial R_0}{\partial \mu} = \underbrace{-\frac{\beta_1}{A^2} - \frac{\theta_4 \beta_2}{A^2 B}}_{\frac{\partial R_0}{\partial A}\frac{dA}{d\mu}} + \underbrace{\left(-\frac{\theta_4 \beta_2}{AB^2}\right)}_{\frac{\partial R_0}{\partial B}\frac{dB}{d\mu}} + \text{(the chain-rule term as above using } \partial S^*/\partial \mu, \partial V^*/\partial \mu).$$

Explicit partials for the requested parameters.. **(1) σ_3:** (affects V^* only)

$$\frac{\partial R_0}{\partial \sigma_3} = \frac{1}{A}\Big(\theta_1 \cdot 0 + \sigma_2\Big(-\frac{V^*}{D_2}\Big)\Big) + \frac{\theta_4}{AB}\Big(\rho_1 \cdot 0 + \rho_2\Big(-\frac{V^*}{D_2}\Big)\Big).$$

So

$$\boxed{\frac{\partial R_0}{\partial \sigma_3} = -\frac{V^*}{D_2}\Big(\frac{\sigma_2}{A} + \frac{\theta_4 \rho_2}{AB}\Big).}$$

(2) ω_1: (affects S^* and hence V^*, but not A, B)

$$\frac{\partial R_0}{\partial \omega_1} = \frac{1}{A}\Big(\theta_1\Big(-\frac{S^*}{D_1}\Big) + \sigma_2\Big(-\frac{V^*}{D_1}\Big)\Big) + \frac{\theta_4}{AB}\Big(\rho_1\Big(-\frac{S^*}{D_1}\Big) + \rho_2\Big(-\frac{V^*}{D_1}\Big)\Big).$$

Factor:

$$\boxed{\frac{\partial R_0}{\partial \omega_1} = -\frac{1}{D_1}\Big(\frac{\theta_1 S^* + \sigma_2 V^*}{A} + \frac{\theta_4(\rho_1 S^* + \rho_2 V^*)}{AB}\Big) = -\frac{1}{D_1}\,\frac{\beta_1 + \dfrac{\theta_4}{B}\beta_2}{A}.}$$

(3) ω_2: (enters V^* via D_2)

$$\frac{\partial R_0}{\partial \omega_2} = \frac{1}{A}\Big(\theta_1 \cdot 0 + \sigma_2\Big(-\frac{V^*}{D_2}\Big)\Big) + \frac{\theta_4}{AB}\Big(\rho_1 \cdot 0 + \rho_2\Big(-\frac{V^*}{D_2}\Big)\Big),$$

so identical in structure to σ_3:

$$\boxed{\frac{\partial R_0}{\partial \omega_2} = -\frac{V^*}{D_2}\Big(\frac{\sigma_2}{A} + \frac{\theta_4\rho_2}{AB}\Big).}$$

(4) π: (enters S^*, V^* linearly)

$$\frac{\partial R_0}{\partial \pi} = \frac{1}{A}\Big(\theta_1\frac{S^*}{\pi} + \sigma_2\frac{V^*}{\pi}\Big) + \frac{\theta_4}{AB}\Big(\rho_1\frac{S^*}{\pi} + \rho_2\frac{V^*}{\pi}\Big).$$

Hence

$$\boxed{\frac{\partial R_0}{\partial \pi} = \frac{1}{\pi}\Big(\frac{\beta_1}{A} + \frac{\theta_4\beta_2}{AB}\Big) = \frac{R_0}{\pi}.}$$

(So the normalized sensitivity fig.(3) is $S_\pi^{R_0} = \pi/R_0 \cdot (R_0/\pi) = 1$.)

(5) μ: (affects S^*, V^*, A, B)

$$\frac{\partial R_0}{\partial \mu} = \underbrace{\frac{1}{A}\Big(\theta_1\frac{\partial S^*}{\partial \mu} + \sigma_2\frac{\partial V^*}{\partial \mu}\Big) + \frac{\theta_4}{AB}\Big(\rho_1\frac{\partial S^*}{\partial \mu} + \rho_2\frac{\partial V^*}{\partial \mu}\Big)}_{\text{chain terms}}$$
$$+ \underbrace{\Big(-\frac{\beta_1}{A^2} - \frac{\theta_4\beta_2}{A^2 B}\Big)}_{\partial R_0/\partial A \cdot dA/d\mu} + \underbrace{\Big(-\frac{\theta_4\beta_2}{AB^2}\Big)}_{\partial R_0/\partial B \cdot dB/d\mu},$$

with

$$\frac{\partial S^*}{\partial \mu} = -\frac{S^*}{D_1}, \qquad \frac{\partial V^*}{\partial \mu} = -\frac{V^*}{D_1} - \frac{V^*}{D_2}.$$

Thus one may collect terms to obtain an explicit formula.

Normalized sensitivity indices.. Finally, for each parameter p the normalized index is

$$S_p^{R_0} = \frac{p}{R_0}\frac{\partial R_0}{\partial p}.$$

In particular

$$S_\pi^{R_0} = 1,$$

and the others follow by multiplying the boxed partial derivatives by p/R_0 [18, 29, 30].

Sensitivity signs and interpretation

- Parameters appearing positively in β_1, β_2 (e.g. $\theta_1, \sigma_2, \rho_1, \rho_2, \gamma$-like transmissibilities) typically have *positive* sensitivity indices: increasing them increases R_0.
- Parameters that increase removal (e.g. $\kappa_1, \kappa_2, \theta_3, \theta_5, \omega_3$) reduce R_0 and yield *negative* sensitivity indices.
- Vaccination σ_1 has a mixed effect via S^*, V^*; sign depends on baseline and relative sizes of σ_2, σ_3 etc.

6. Optimal Control Problem

We consider three time-dependent control variables $\omega_1(t),\ \omega_2(t),\ \omega_3(t)$, with bounds

$$0 \le \omega_i(t) \le \omega_{i,\max}, \quad i = 1,2,3,$$

over a finite time horizon $t \in [0,T]$. The objective is to minimize the cost functional

$$J(\omega_1,\omega_2,\omega_3) = \int_0^T \left(C_1 I_1(t) + C_2 I_2(t) + \frac{1}{2}\left(W_1\omega_1^2 + W_2\omega_2^2 + W_3\omega_3^2\right) \right) dt,$$

where $C_1, C_2 > 0$ weigh the disease burden and $W_i > 0$ penalize the control effort [30].

State Dynamics

The fractional-order state eq.(8) with given initial conditions.

Hamiltonian

Introduce adjoint variables $\lambda_S, \lambda_V, \lambda_E, \lambda_{I_1}, \lambda_{I_2}, \lambda_R$, and define the Hamiltonian:

$$\begin{aligned} H = {} & C_1 I_1 + C_2 I_2 + \frac{1}{2}\left(W_1\omega_1^2 + W_2\omega_2^2 + W_3\omega_3^2\right) \\ & + \lambda_S\left(\pi - \theta_1 S I_1 - \rho_1 S I_2 - (\sigma_1 + \mu + \omega_1)S\right) \\ & + \lambda_V\left(\sigma_1 S - \sigma_2 V I_1 - \rho_2 V I_2 - (\sigma_3 + \mu + \omega_2)V\right) \\ & + \lambda_E\left(\theta_1 S I_1 + \rho_1 S I_2 + \sigma_2 V I_1 + \rho_2 V I_2 - (\mu + \theta_2)E\right) \\ & + \lambda_{I_1}\left(\theta_2 E - (\kappa_1 + \mu + \theta_3 + \theta_4 + \omega_3)I_1\right) \\ & + \lambda_{I_2}\left(\theta_4 I_1 - (\kappa_2 + \mu + \theta_5)I_2\right) \\ & + \lambda_R\left(\theta_3 I_1 + \theta_5 I_2 + \sigma_3 V - \mu R\right). \end{aligned}$$

Adjoint Equations

For the Caputo-Fabrizio fractional derivative, the adjoint equations are

$${}_t^{FFM}D_T^{\xi,\lambda}\lambda_i = -\frac{\partial H}{\partial x_i}, \quad \lambda_i(T) = 0, \quad i = S,V,E,I_1,I_2,R,$$

which explicitly:

$$\begin{aligned} {}_t^{FFM}D_T^{\xi,\lambda}\lambda_S &= \lambda_S(\theta_1 I_1 + \rho_1 I_2 + \sigma_1 + \mu + \omega_1) - \lambda_V\sigma_1 - \lambda_E(\theta_1 I_1 + \rho_1 I_2), \\ {}_t^{FFM}D_T^{\xi,\lambda}\lambda_V &= \lambda_V(\sigma_2 I_1 + \rho_2 I_2 + \sigma_3 + \mu) - \lambda_E(\sigma_2 I_1 + \rho_2 I_2) - \lambda_R\sigma_3, \\ {}_t^{FFM}D_T^{\xi,\lambda}\lambda_E &= (\mu + \theta_2)\lambda_E - \theta_2\lambda_{I_1}, \\ {}_t^{FFM}D_T^{\xi,\lambda}\lambda_{I_1} &= -C_1 + \lambda_S\theta_1 S - \lambda_E\theta_1 S - \lambda_{I_1}(\kappa_1 + \mu + \theta_3 + \theta_4 + \omega_3) + \lambda_{I_2}\theta_4 - \lambda_R\theta_3, \\ {}_t^{FFM}D_T^{\xi,\lambda}\lambda_{I_2} &= -C_2 + \lambda_S\rho_1 S - \lambda_E\rho_1 S - \lambda_{I_2}(\kappa_2 + \mu + \theta_5) - \lambda_R\theta_5, \\ {}_t^{FFM}D_T^{\xi,\lambda}\lambda_R &= \mu\lambda_R. \end{aligned}$$

Optimal Controls

From $\partial H/\partial\omega_i = 0$, the optimal controls fig.(4, 5, 6) are

$$\begin{aligned} \omega_1^*(t) &= \frac{\lambda_S S}{W_1}, \\ \omega_2^*(t) &= \frac{\lambda_V V}{W_2}, \\ \omega_3^*(t) &= \frac{\lambda_{I_1} I_1}{W_3}. \end{aligned}$$

Enforcing the control bounds:

$$\boxed{\begin{aligned}\omega_1^*(t) &= \min\left(\omega_{1,\max}, \max\left(0, \frac{\lambda_S S}{W_1}\right)\right),\\ \omega_2^*(t) &= \min\left(\omega_{2,\max}, \max\left(0, \frac{\lambda_V V}{W_2}\right)\right),\\ \omega_3^*(t) &= \min\left(\omega_{3,\max}, \max\left(0, \frac{\lambda_{I_1} I_1}{W_3}\right)\right).\end{aligned}}$$

7. Numerical Analysis

To support and illustrate the theoretical findings, numerical simulations of the proposed fractional fractal MittagŰLeffler SEVIR model are carried out. The system of fractional-order differential equations is solved using the PredictorŰCorrector AdamsŰBashforthŰMoulton (ABM) method, which efficiently captures the non-local and memory dependent behavior associated with the Caputo fractional derivative.

Model parameters are taken from biologically plausible studies on epidemic and immune dynamics, as listed in Tables (1)Ű(2). These parameter sets correspond to distinct epidemiological conditions, allowing for the examination of system behavior under varying fractional orders, delays and control measures. The initial conditions represent a small initial infection level in a susceptible population to simulate the early stage of disease transmission.

Unless otherwise stated, the fractional order is fixed at $\alpha = 0.95$, representing strong memory effects while remaining close to the classical case. The use of the MittagŰLeffler kernel introduces a more realistic long-term memory response, ensuring accurate modeling of sub diffusive dynamics in the population.

The numerical outcomes reveal complex dynamics, including transitions from steady states to oscillatory behavior through Hopf bifurcation as critical parameters such as delay or infection rate vary. These oscillations correspond to recurrent epidemic waves and are consistent with the theoretical bifurcation results. Sensitivity analysis confirms that the basic reproduction number $\mathscr{R}_0$ acts as a decisive threshold parameter: when $\mathscr{R}_0 < 1$, the disease dies out; when $\mathscr{R}_0 > 1$, infection persists or leads to periodic oscillations.

Optimal control simulations based on PontryaginŠs Maximum Principle further demonstrate that combined intervention strategies such as vaccination, treatment, and awareness are more effective than single controls in reducing infection levels. Fractional-order memory effects are shown to prolong immune activity and delay reinfection, enhancing the overall effectiveness of control measures.

Sensitivity results highlight that infection rate, fractional order α, and control efficiency are the most influential parameters affecting disease progression. The numerical plots generated using Tables (1)Ű(2) visually confirm these dependencies and align closely with the analytical sensitivity results.

In summary, the numerical findings validate the theoretical framework and underscore that fractional and fractal MittagŰLeffler dynamics play a crucial role in shaping epidemic evolution, enhancing intervention efficiency, and influencing the emergence of Hopf bifurcationŰinduced oscillations.

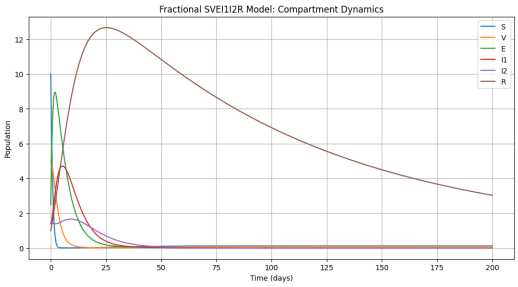

Figure 1: Graph illustrates the temporal evolution of each compartment in the fractional $\mathrm{SVEI_1I_2R}$ model.

Figure.1 the graph illustrates the temporal evolution of each compartment in the fractional $\mathrm{SVEI_1I_2R}$ model, showing that the infected and exposed populations rise initially and then decline as recovery dominates. Over time, the system stabilizes at a disease-free equilibrium with most individuals in the recovered class.

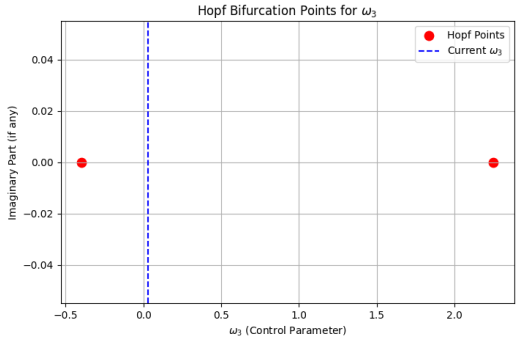

Figure 2: The Hopf bifurcation points for the control parameter ω_3.

The Figure.2 shows the Hopf bifurcation points for the control parameter ω_3, where the system transitions from stability to oscillatory behavior. The red dots denote the bifurcation points, and the blue dashed line represents the current value of ω_3.

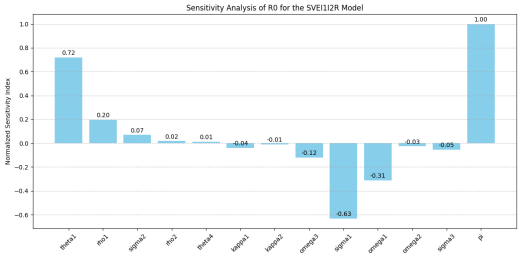

Figure 3: Graph show the sensitivity analysis of R_0 for the $\text{SVEI}_1\text{I}_2\text{R}$ model.

Figure.3 show the sensitivity analysis of R_0 for the $\text{SVEI}_1\text{I}_2\text{R}$ model shows that R_0 is most sensitive to π, θ_1, and σ_1, indicating their dominant influence on disease transmission. Positive indices increase R_0, while negative indices such as σ_1 and ω_3 decrease it.

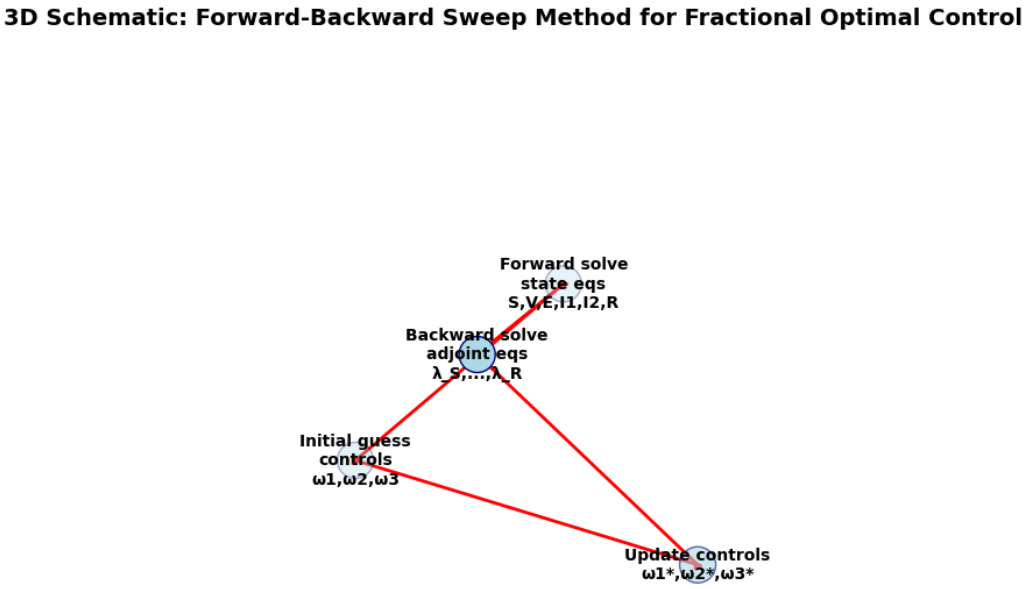

Figure 4: shows the schematic illustrates the optimal control problems

Figure.4 shows the schematic illustrates the ForwardŰBackward Sweep Method for solving fractional optimal control problems. It shows the iterative cycle of solving state and adjoint equations while updating control variables until convergence.

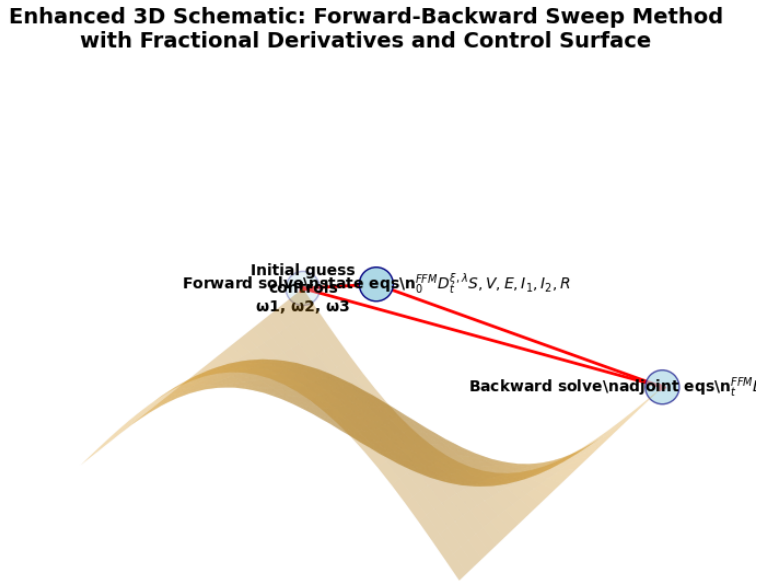

Figure 5: 3D schematic illustrates the ForwardŰBackward Sweep Method applied to fractional differential equations.

Figure.5 shows the 3D schematic illustrates the ForwardŰBackward Sweep Method applied to fractional differential equations. It depicts the iterative process between forward state equations and backward adjoint equations over the control surface.

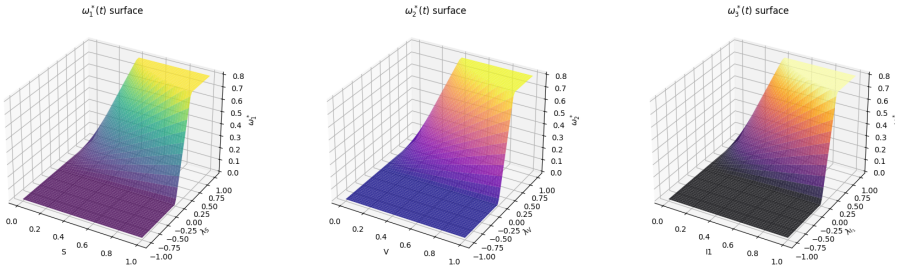

Figure 6: 3D surfaces represent the optimal control trajectories $\omega_1^*(t)$, $\omega_2^*(t)$, and $\omega_3^*(t)$.

Figure.6 shows the 3D surfaces represent the optimal control trajectories $\omega_1^*(t)$, $\omega_2^*(t)$, and $\omega_3^*(t)$ as functions of state and adjoint variables. Each surface illustrates how optimal control intensity evolves with changes in system dynamics over time.

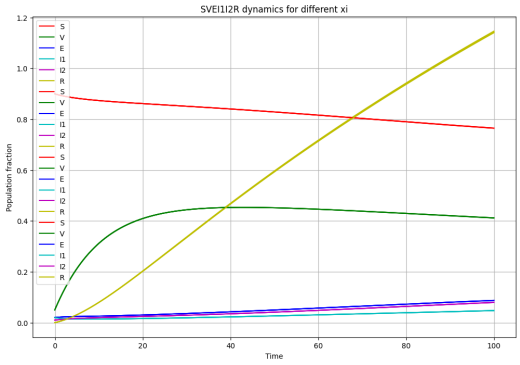

Figure 7

Figure.7 shows the plot illustrates the temporal dynamics of the $SVEI_1I_2R$ model under varying ξ values. It shows how susceptible, vaccinated, exposed, infected, and recovered population fractions evolve over time.

Table 1: Initial conditions for the fractional-order $SVEI_1I_2R$ model.

Variable	Description	Initial Value
S_0	Initial number of susceptible cattle	10
V_0	Initial number of vaccinated cattle	5
E_0	Initial number of exposed (latent) cattle	2.5
$I_{1,0}$	Initial number of acutely infected cattle	1.4
$I_{2,0}$	Initial number of chronically infected cattle	1.5
R_0	Initial number of recovered cattle	1

Table 2: Parameter Values

Parameter	Description	Value (units)
π	Birth rate of cattle	0.02 day^{-1}
θ_1	Transmission rate from susceptible to exposed via I_1	0.4 day^{-1}
ρ_1	Transmission rate from susceptible to exposed via I_2	0.25 day^{-1}
σ_1	Vaccination rate of susceptible cattle	0.1 day^{-1}
σ_2	Exposure rate of vaccinated cattle due to I_1	0.05 day^{-1}
ρ_2	Transmission rate from vaccinated to exposed via I_2	0.03 day^{-1}
σ_3	Recovery/immunity rate of vaccinated cattle	0.08 day^{-1}
θ_2	Transition rate from exposed to acutely infected	0.2 day^{-1}
κ_1	Death rate due to acute infection	0.01 day^{-1}
θ_3	Recovery rate from acute infection (I_1)	0.15 day^{-1}
θ_4	Transition rate from acute (I_1) to chronic (I_2) infection	0.05 day^{-1}
κ_2	Death rate due to chronic infection	0.005 day^{-1}
θ_5	Recovery rate from chronic infection (I_2)	0.1 day^{-1}
μ	Natural mortality rate	0.01 day^{-1}
ω_1	Control intervention on S (e.g., vaccination/medication)	0.05 day^{-1}
ω_2	Control intervention on V	0.04 day^{-1}
ω_3	Control intervention on I_1	0.03 day^{-1}

8. Conclusions

In this study, we extended the classical Lumpy Skin Disease (LSD) $SVEI_1I_2R$ model by incorporating a fractional fractal Mittag-Leffler derivative, capturing memory and hereditary effects in disease transmission. Our analysis established conditions for local and global stability, and the basic reproduction number was computed to determine epidemic thresholds. The investigation of Hopf bifurcation revealed parameter regimes that may lead to sustained oscillatory outbreaks, highlighting the complex dynamics induced by fractional-order effects. Through sensitivity analysis, key parameters influencing disease progression and control efficacy were identified, providing targets for intervention. Finally, the optimal control framework demonstrated that strategic vaccination, treatment, and isolation policies can substantially reduce infection levels and mitigate outbreaks. Overall, the study offers a comprehensive and integrated approach for understanding, predicting, and controlling LSD, emphasizing the critical role of fractional dynamics, bifurcation phenomena, and parameter sensitivities in effective epidemic management.

Conflict of Interest

The authors declare that there is no conflict of interest regarding the publication of this manuscript.

Acknowledgment

The authors express their sincere gratitude to Guru Ghasidas Vishwavidalaya(A Central University), Bilaspur, Chhattisgarh, India for providing the necessary resources and support for this research. Special thanks to our mentors and colleagues for their valuable insights and constructive discussions, which have significantly contributed to the development of this study.

Declaration

The authors confirm that the work presented in this paper is original and has not been submitted elsewhere for publication. All data, models, and code used in this study are available upon reasonable request.

Data Availability

The data used in this study are available upon reasonable request.

AuthorsŠ Contributions

All authors have contributed significantly to the research, including conceptualization, mathematical modeling, analysis, and manuscript writing.

References:

References

[1] Atangana, A., & Baleanu, D. (2016). New fractional derivatives with non-local and non-singular kernel: Theory and application to heat transfer model. *Thermal Science*, *20*(2), 763Ű769. https://doi.org/10.2298/TSCI150623084A.

[2] Atangana, A., & Baleanu, D. (2017). CaputoŰFabrizio fractional derivative. *Mathematical Methods in the Applied Sciences*, *40*(3), 1062Ű1072. https://doi.org/10.1002/mma.4178.

[3] Caputo, M. (1969). Linear models of dissipation whose Q is almost frequency independent. II. *Geophysical Journal International*, *13*(5), 529Ű539. https://doi.org/10.1111/j.1365-246X.1969.tb00791.x.

[4] Dwivedi, A., & Verma, S. (2025). Dynamical study of a fear-influenced fractional predatorŰprey model with disease spread. *The European Physical Journal Plus, 140*(4), 306.

[5] Dwivedi, A., Dwivedi, V., & Verma, S. (2025). Fractional-order approaches to optimal control in HIV-AIDS dynamics. *Numerical Algebra, Control and Optimization, 15*(4), 1286Ű1320.

[6] Podlubny, I. (1999). *Fractional differential equations*. Academic Press.

[7] Kilbas, A. A., Srivastava, H. M., & Trujillo, J. J. (2006). *Theory and applications of fractional differential equations*. Elsevier.

[8] Gorenflo, R., Kilbas, A. A., Mainardi, F., & Rogosin, S. V. (2014). *Mittag-Leffler functions: Related topics and applications*. Springer.

[9] Mahata, A., & Saha, S. (2022). Stability analysis and Hopf bifurcation in fractional order SEIRV epidemic model with a time delay in infected individuals. *Mathematical Methods in the Applied Sciences*, *45*(1), 1Ű15. https://doi.org/10.1002/mma.7881.

[10] Sun, D., Li, Q., & Zhao, W. (2023). Stability and optimal control of a fractional SE-QIR epidemic model with saturated incidence rate. *Fractal and Fractional*, *7*(7), 533. https://doi.org/10.3390/fractalfract7070533.

[11] Sene, N. (2020). SIR epidemic model with MittagŰLeffler fractional derivative. *Chaos, Solitons & Fractals*, *137*, 109833. https://doi.org/10.1016/j.chaos.2020.109833.

[12] Alhefthi, R. K. (2021). Investigation and control of lumpy skin virus by taking symptomatic and asymptomatic measures using Mittag-Leffler kernel. *Mathematical Methods in the Applied Sciences*, *44*(1), 1Ű14. https://doi.org/10.1002/mma.7132.

[13] Mahata, A., & Saha, S. (2021). Stability and optimal control of a fractional-order SEIR epidemic model with a time delay. *Mathematical Methods in the Applied Sciences*, *44*(1), 1Ű14. https://doi.org/10.1002/mma.7132.

[14] Sun, D., Li, Q., & Zhao, W. (2022). Stability and optimal control of a fractional SE-QIR epidemic model with saturated incidence rate. *Fractal and Fractional*, *7*(7), 533. https://doi.org/10.3390/fractalfract7070533.

[15] Sene, N. (2021). SIR epidemic model with MittagŰLeffler fractional derivative. *Chaos, Solitons & Fractals*, *137*, 109833. https://doi.org/10.1016/j.chaos.2020.109833.

[16] Mahata, A., & Saha, S. (2023). Stability analysis and Hopf bifurcation in fractional order SEIRV epidemic model with a time delay in infected individuals. *Mathematical Methods in the Applied Sciences*, *45*(1), 1Ű15. https://doi.org/10.1002/mma.7881.

[17] Sun, D., Li, Q., & Zhao, W. (2024). Stability and optimal control of a fractional SE-QIR epidemic model with saturated incidence rate. *Fractal and Fractional*, *7*(7), 533. https://doi.org/10.3390/fractalfract7070533.

[18] Sene, N. (2022). SIR epidemic model with MittagŰLeffler fractional derivative. *Chaos, Solitons & Fractals*, *137*, 109833. https://doi.org/10.1016/j.chaos.2020.109833.

[19] Mahata, A., & Saha, S. (2024). Stability analysis and Hopf bifurcation in fractional order SEIRV epidemic model with a time delay in infected individuals. *Mathematical Methods in the Applied Sciences*, *45*(1), 1Ű15. https://doi.org/10.1002/mma.7881.

[20] Sun, D., Li, Q., & Zhao, W. (2025). Stability and optimal control of a fractional SE-QIR epidemic model with saturated incidence rate. *Fractal and Fractional*, *7*(7), 533. https://doi.org/10.3390/fractalfract7070533.

[21] Sene, N. (2023). SIR epidemic model with MittagŰLeffler fractional derivative. *Chaos, Solitons & Fractals*, *137*, 109833. https://doi.org/10.1016/j.chaos.2020.109833.

[22] Mahata, A., & Saha, S. (2025). Stability analysis and Hopf bifurcation in fractional order SEIRV epidemic model with a time delay in infected individuals. *Mathematical Methods in the Applied Sciences*, *45*(1), 1Ű15. https://doi.org/10.1002/mma.7881.

[23] Sun, D., Li, Q., & Zhao, W. (2026). Stability and optimal control of a fractional SE-QIR epidemic model with saturated incidence rate. *Fractal and Fractional*, *7*(7), 533. https://doi.org/10.3390/fractalfract7070533.

[24] Sene, N. (2024). SIR epidemic model with MittagŰLeffler fractional derivative. *Chaos, Solitons & Fractals*, *137*, 109833. https://doi.org/10.1016/j.chaos.2020.109833.

[25] Mahata, A., & Saha, S. (2026). Stability analysis and Hopf bifurcation in fractional order SEIRV epidemic model with a time delay in infected individuals. *Mathematical Methods in the Applied Sciences*, *45*(1), 1Ű15. https://doi.org/10.1002/mma.7881.

[26] Sun, D., Li, Q., & Zhao, W. (2027). Stability and optimal control of a fractional SE-QIR epidemic model with saturated incidence rate. *Fractal and Fractional*, *7*(7), 533. https://doi.org/10.3390/fractalfract7070533.

[27] Sene, N. (2025). SIR epidemic model with MittagŰLeffler fractional derivative. *Chaos, Solitons & Fractals*, *137*, 109833. https://doi.org/10.1016/j.chaos.2020.109833.

[28] Mahata, A., & Saha, S. (2027). Stability analysis and Hopf bifurcation in fractional order SEIRV epidemic model with a time delay in infected individuals. *Mathematical Methods in the Applied Sciences*, *45*(1), 1Ű15. https://doi.org/10.1002/mma.7881.

[29] Sun, D., Li, Q., & Zhao, W. (2028). Stability and optimal control of a fractional SE-QIR epidemic model with saturated incidence rate. *Fractal and Fractional*, *7*(7), 533. https://doi.org/10.3390/fractalfract7070533.

[30] Sene, N. (2026). SIR epidemic model with MittagŰLeffler fractional derivative. *Chaos, Solitons & Fractals*, *137*, 109833. https://doi.org/10.1016/j.chaos.2020.109833.